The Journal of Experimental Biology 216, 2741-2751

doi:10.1242/jeb.081984

RESEARCH ARTICLE

The physiological response of the marine platyhelminth *Macrostomum lignano* to different environmental oxygen concentrations

G. A. Rivera-Ingraham[1,*], U. Bickmeyer[2] and D. Abele[1]

[1]Department of Functional Ecology and [2]Department of Ecological Chemistry, Alfred Wegener Institute, Helmholtz Centre for Polar and Marine Research, Am Handelshafen 12, 27570 Bremerhaven, Germany

*Author for correspondence (Georgina.Rivera-Ingraham@awi.de)

SUMMARY

The respiration rate of meiofauna is difficult to measure, and the response to variations in the environmental oxygen concentration has so far been mainly addressed through behavioral investigation. We investigated the effect of different oxygen concentrations on the physiology of the marine platyhelminth *Macrostomum lignano*. Respiration was measured using batches of 20 animals in a glass microtiter plate equipped with optical oxygen sensor spots. At higher oxygen saturations (>12 kPa), the animals showed a clear oxyconforming behavior. However, below this value, the flatworms kept respiration rates constant at 0.064±0.001 nmol O_2 l^{-1} h^{-1} $individual^{-1}$ down to 3 kPa P_{O_2}, and this rate was increased by 30% in animals that were reoxygenated after enduring a period of 1.5 h in anoxia. Physiological changes related to tissue oxygenation were assessed using live imaging techniques with different fluorophores in animals maintained in normoxic (21 kPa), hyperoxic (40 kPa) or near-anoxic (~0 kPa) conditions and subjected to anoxia–reoxygenation. The pH-sensitive dyes Ageladine-A and BCECF both indicated that pH_i under near-anoxia increases by about 0.07–0.10 units. Mitochondrial membrane potential, $\Delta\psi_m$, was higher in anoxic and hyperoxic than in normoxic conditions (JC1 dye data). Staining with ROS-sensitive dyes – DHE for detection of superoxide anion ($O_2^{\bullet-}$) formation and C-H_2DFFDA for other ROS species aside from $O_2^{\bullet-}$ (H_2O_2, HOO• and $ONOO^-$) – showed increased ROS formation following anoxia–reoxygenation treatment. Animals exposed to hyperoxic, normoxic and anoxic treatments displayed no significant differences in $O_2^{\bullet-}$ formation, whereas mitochondrial ROS formation as detected by C-H_2DFFDA was higher after hyperoxic exposure and lowest under near-anoxia conditions compared with the normoxic control group. *Macrostomum lignano* seems to be a species that is tolerant of a wide range of oxygen concentrations (being able to maintain aerobic metabolism from extremely low P_{O_2} up to hyperoxic conditions), which is an essential prerequisite for successfully dealing with the drastic environmental oxygen variations that occur within intertidal sediments.

Supplementary material available online at http://jeb.biologists.org/cgi/content/full/216/14/2741/DC1

Key words: flatworm, live imaging, meiofauna, respiration.

Received 23 October 2012; Accepted 7 March 2013

INTRODUCTION

Marine meiofauna colonize the upper sediment layer of the ocean, which, especially in coastal and intertidal sediments, can be highly variable with respect to oxygenation. On the one hand, wave action and coastal currents often lead to mechanical mixing of oxygen-rich surface water into the upper loosely packed sediment layers. Relatively compacted sediment surfaces in shallow waters are often densely colonized by benthic microalgae that cause daily peaks of photosynthetic oxygenation in the upper 1–2 cm of sediment surface. On the other hand, coastal sediments contain high amounts of organic matter from decaying macroalgae or terrestrial and riverine coastal runoff. The chemical and microbial oxygen demand in these sediments is high so that oxygen that diffuses downwards is rapidly consumed. This produces steep sedimentary redox gradients between the upper, sometimes even hyperoxic and the lower suboxic to anoxic layers, which often span no more than 10–50 cm, below which the sediment becomes chronically anoxic and sulfidic (rich in hydrogen sulfide, H_2S) (Fenchel and Finlay, 2008). These sediments are colonized by highly diverse macrofauna and meiofauna communities, the composition of which varies depending on sediment stability, grain size composition, organic matter content and oxygenation. Whereas macrofauna organisms often build sedimentary burrows that they oxygenate through irrigation with oxygen-rich surface waters, meiofauna organisms move between the sand grains, seeking optimal positioning between too high and too low environmental oxygenation according to their metabolic and nutritional requirements. In very few cases were marine meiofauna found to actively establish suitable environmental oxygen levels in their closest environment between the sediment grains (Corbari et al., 2005). Much more often it was shown that the meiofauna stratify in response to the sedimentary oxygen gradient (Corbari et al., 2004) and different groups of meiofauna have been described as oxophilic, microoxophilic and thiobiotic according to their preferred positioning in the small-scale chemical and redox gradients within the sediment column and around macrofauna burrows (Fenchel and Finlay, 1995; Morrill et al., 1988). This behavior precludes not only that meiofauna species have different metabolic strategies to cope with low and variable environmental oxygenation but also that they would have the means to sense oxygen (and hydrogen sulfide) and react flexibly to changing environmental oxygenation. These reactions include vertical migrations within the sediment column, often away from the too high surface oxygenation (Corbari et al., 2005), and/or adjustment of

metabolic rate to cope with reduced oxygen availability. However, soft-bodied meiofauna worms, such as nematodes and platyhelminths, generally deal with fluctuating tissue oxygenation and changes in environmental redox state because of their small size and fast equilibration time. Whereas several studies have assessed the behavioral (Rosenberg et al., 1991; Tinson and Laybourn-Parry, 1985) and ecological responses to fluctuating oxygenation (Wetzel et al., 2001), studies of the physiological response to fluctuating chemical and oxygenation gradients are scarce.

A seminal paper by Morrill and colleagues (Morrill et al., 1988) reported antioxidant activities to be better established in thiobiotic than in oxybiotic meiofauna, giving rise to the idea that (i) normoxic oxygen levels could already be 'hyperoxic' for these low oxygen-adapted species, and (ii) the oxidation of toxic H_2S could give rise to the formation of reactive oxygen species (ROS) in thiobiotic, low oxygen-adapted meiofauna.

In the present study, we investigated the physiological effects of hyperoxic and anoxic exposure conditions in the interstitial marine flatworm *Macrostomum lignano* (Rhabditophora, Macrostomorpha) (Ladurner et al., 2005). *Macrostomum lignano* has been established as a new model in sexual selection (Schärer et al., 2005) and evolutionary and developmental studies (Egger et al., 2006; Morris et al., 2006), but especially in stem-cell research (Bode et al., 2006; Pfister et al., 2007) and the role of these stem-cells in the process of aging (Mouton et al., 2009).

Platyhelminths are transparent and, thus, elegant model organisms to study cellular and subcellular processes *in vivo*. Using 'live imaging' techniques we provide a first set of data regarding the physiological responses of individual flatworms to extreme states of environmental oxygenation and, further, on the effect of anoxia and subsequent reoxygenation on ROS-forming processes, mitochondrial membrane potential (ψ_m) and tissue pH. We developed a technique to record oxygen partial pressure (P_{O_2})-dependent oxygen consumption rates using batches of 20 flatworms in order to describe their metabolic response to variable environmental oxygenation.

In this study we used non-invasive optical techniques to understand how an anoxia-tolerant animal responds to high, low and fluctuating oxygenation, especially with respect to ROS formation, mitochondrial functioning and maintenance pH homeostasis during anoxia–reoxygenation, a detrimental situation in many human pathologies.

MATERIALS AND METHODS

Animal culturing

Cultures of *M. lignano* (DV-1 line) were reared at the Alfred Wegener Institute (Bremerhaven, Germany) in Petri dishes with Guillard's F/2 medium at room temperature (RT, 20°C) and fed weekly with the diatom *Nitzschia* sp. For experimentation, however, a sterile medium composed of seawater filtered through a 0.2 μm Whatman filter and supplemented with 15 mmol l^{-1} Na-Hepes (NH-FSW) was used. Buffering was necessary to avoid pH changes in the medium when setting anoxic or hyperoxic conditions.

Respiration measurements

Two different treatments were considered for the respiration measurements: normoxia (21 kPa) and anoxia (0 kPa) followed by reoxygenation. For the latter, animals were kept for 1.5 h under anoxic conditions (in a gas-tight glovebox that was equilibrated with 100% N_2 and immersed in an anoxic medium, prepared by flushing with 100% N_2) and later reoxygenated by bubbling with air for an additional 1.5 h. Prior to the respiration measurements, experimental animals were isolated from the cultures and maintained without food for *ca*. 20 h in NH-FSW. After this acclimation time, three groups of 20 animals were transferred with a micropipette to three individual wells of a glass microtiter plate (Mikroglas Chemtech, Mainz, Germany) previously equipped with oxygen sensor spots (SP-PSt3-NAU-D5-YOP, Precision Sensing, Regensburg, Germany) glued onto the bottom of each well. An additional well was maintained as a control, and contained only NH-FSW and the sensor spot. Each of the wells was filled completely with NH-FSW to its maximum capacity, which was 100±0.5 μl, to avoid the formation of air bubbles when sealing the wells. Each of the four wells was sealed with a coverslip and the complete surface of the microtiter plate was additionally covered with a layer of auto-adhesive Armaflex (Armacell Enterprise, Münster, Germany). Additional pressure was maintained on the complete surface of the plate in order to ensure air-tight sealing. Measurements were carried out with a four-channel fiber-optic oxygen meter (Oxy-4) and non-invasive oxygen sensors (Precision Sensing), which were daily calibrated following the manufacturer's description. Data were recorded at 15 s intervals and the experiments were stopped when the oxygen was completely consumed from each of the animal chambers, which usually took around 16 h. All experiments were conducted at RT. Data corresponding to the first 30 min following the start of the experiment were discarded in order to avoid interference from stress related to the manipulation of the worms. Respiration rates were expressed as nmol $O_2\,l^{-1}\,h^{-1}$ individual^{-1}. The critical oxygen partial pressure (P_c) (Tang, 1933) was calculated using the equation of Duggleby (Duggleby, 1984).

Optical measurements

In this study, intracellular pH (pH_i), ψ_m, mitochondrial density and ROS concentration were measured by 'live imaging' techniques, involving the application of specific dyes and *in vivo* visualization using a Leica TCS SP5II confocal microscope (Leica Microsystems CMS, Wetzlar, Germany) and a CCD camera system (Visitron Systems, Puchheim, Germany).

Four treatments were considered in our study: control (21 kPa), anoxia (0 kPa), hyperoxia (40 kPa) and anoxia followed by reoxygenation. Experiments were carried out in a gas-tight glovebox, which was equilibrated with either 100% N_2 (anoxia) or 40% O_2/60% N_2 (hyperoxia) using a Wösthoff gas-mixing pump (Wösthoff, Bochum, Germany). Anoxic medium was prepared by flushing with 100% N_2, while hyperoxic NH-FSW medium was obtained by flushing with a 40% O_2–60% N_2 mixture; flushing for 30 min was enough for equilibration in all cases, as confirmed by measurement of the oxygen content using optical oxygen sensors and the Presens Oximeter (see above).

Treatments were conducted with batches of 10 animals that were manipulated at the same time in 2 ml Utermöhl chambers for 1.5 h. The microscopic chamber in which the animals were anoxically incubated was sealed while still inside the glovebox and under the gas stream. The chamber was then transferred to the confocal microscope. For the anoxic treatment, it should be noted that we cannot exclude some minor reoxygenation; thus, we decided to use the term 'near-anoxia' for the treatment that was aimed to be strictly anoxia. At the end of the incubation, a fluorophore was added to the animals in normoxic, anoxic (severely hypoxic) and hyperoxic treatments.

For the anoxia–reoxygenation treatment, the worms were incubated in absolute anoxia; the chamber was subsequently opened and medium and animals were allowed to reoxygenate for an additional 1.5 h. After this time, the dye was added to the

Table 1. Description of the dyes used during the present study

Dye	Parameter measured	Company/code	Mechanism of function
Ageladine-A (in DMSO)	pH	*	Probe that exists as a nearly uncharged monomer at pH 8.1–8.6. After crossing cellular membranes, it becomes charged in the cytosol and acidic compartments of cells.
BCECF AM (in DMSO)	pH	Molecular Probes (B-3051)	Probe that shows an absorption shift depending on whether it is in the basic (phenolate anion) or acidic (protonated) form.
MitoTracker Green FM (in DMSO)	Mitochondrial density	Molecular Probes (M-7514)	Non-fluorescent molecule that becomes fluorescent once it accumulates in the lipid environment of the mitochondria.
MitoTracker Deep Red 633 (in DMSO)	Mitochondrial density	Molecular Probes (M-22426)	Non-fluorescent molecule that becomes fluorescent once it accumulates in the lipid environment of the mitochondria.
JC-1 (in DMSO)	Mitochondrial membrane potential	Molecular Probes (T-3168)	Green fluorescent probe that exists as a monomer at low $\Delta\psi_m$. With high $\Delta\psi_m$ values, JC-1 aggregates and shows a red fluorescence.
DHE (in DMSO)	$O_2^{\bullet -}$	Molecular Probes (D-23107)	Regularly shows a blue emission when excited with a 355 nm laser. When oxidized by the presence of O_2^-, it intercalates with the DNA and shows a red emission when excited with an argon laser.
C-H_2DFFDA (in ethanol)	H_2O_2, HOO• and $ONOO^-$	Molecular Probes (C-13293)	Non-fluorescent molecule that is converted to a green fluorescent form when the acetate groups are removed by intracellular esterases and oxidation occurs in the cell.

DHE, dihydroethidium.
*Synthesized by Sudhir R. Shengule and Peter Karuso, Macquarie University, Sydney.

reoxygenation treatment. All dyes were used individually for separate batches of animals in order to avoid any possible interference among dyes. The list of the different dyes used in the present study along with their mechanisms of function is given in Table 1, while incubation and analysis conditions for each of these dyes are detailed in Table 2.

For both of the pH-sensitive dyes used in the present study (Ageladine-A and BCECF), further calibration was needed in order to assign numerical pH values to the experimentally recorded intensities/ratios. For Ageladine-A (Fujita et al., 2003), this was done following a previously described method (Bickmeyer et al., 2008; Bickmeyer, 2012) in which the average values obtained for each of the treatments are expressed as a proportion of the control values, and by assuming that non-specialized cells under these control conditions would present a putative pH_i of 7.3–7.4. In contrast, as BCECF fluorescence intensity at 490 nm linearly increases between pH 6.4 and 7.8 (Silver, 2003), BCECF results were converted to pH_i by constructing a calibration curve using the nigericin technique (nigericin sodium salt, 5 mg, N7143, Sigma-Aldrich, St Louis, MO, USA) described previously (Thomas et al., 1979).

Fluorimetric analysis of the response of the animals to the treatment conditions was carried out in sealed microscope slides using a Leica TCS SP5II confocal microscope. For validation of the pH_i results, further analyses were carried out using a wide-field fluorescence microscope Zeiss Axiovert-10 (Zeiss, Jena, Germany; equipped a CCD camera system, Visitron) and applying BCECF staining. For analysis, animals were anesthetized in a 2:1 mixture of 7.14% $MgCl_2 \cdot 6H_2O$ and NH-FSW (Pfannkuche and Thiel, 1988). One picture per individual and per photomultiplier tube (PMT), when ratio calculation was required, was taken for each of the animals using a 10× objective lens. In order to avoid photobleaching, a short period (<5 s) of low resolution (256×256 pixels) live scanning was applied for focus adjustments and afterwards only one single scan (512×512 pixels) was run of each individual. Autofluorescence was suppressed by adjusting the threshold, and phototoxicity was minimized by the multiphoton laser for low wavelength scans.

Image analysis was carried out using Leica LAS Lite software (Leica Microsystems). Quantification was carried out by plotting five transects per animal (always perpendicular to the longitudinal axis of the animal and in all cases selecting the areas of highest intensity;

Table 2. Analysis conditions for each of the dyes used during the study

Dye	Final concentration (μmol l^{-1})	Incubation time (min)	No. individuals per batch	No. repetitions (total no. individuals)	Excitation wavelength λ_1 (nm)	Excitation wavelength λ_2 (nm)	Emission wavelength PMT1 (nm)	Emission wavelength PMT2 (nm)	Calculation
Ageladine-A (in DMSO)	15	90	10	4 (40)	MP (370)	–	420–500	–	Maximum intensity
BCECF AM (in DMSO)	5.0	90	10	2 (20)	MP (439)	488	520–550	–	Maximum λ_2/λ_1 ratio
MitoTracker Green FM (in DMSO)	0.33	30	10	2 (20)	488	–	500–550	–	Maximum intensity
MitoTracker Deep Red 633 (in DMSO)	0.33	60	10	4 (40)	633	–	640–680	–	Maximum intensity
JC-1 (in DMSO)	5	60	10	2 (20)	488	488	500–550	560–600	PMT1/PMT2 ratio
DHE (in DMSO)	3.3	30	10	3 (30)	MP (355)	488	400–440	620–660	PMT2/PMT1 ratio
C-H_2DFFDA (in ethanol)	10.6	30	10	2 (20)	488	–	510–550	–	Maximum intensity

DHE, dihydroethidium; MP, multiphoton laser; PMT, photomultiplier tube.
Values in parentheses indicate the effective excitation wavelength.

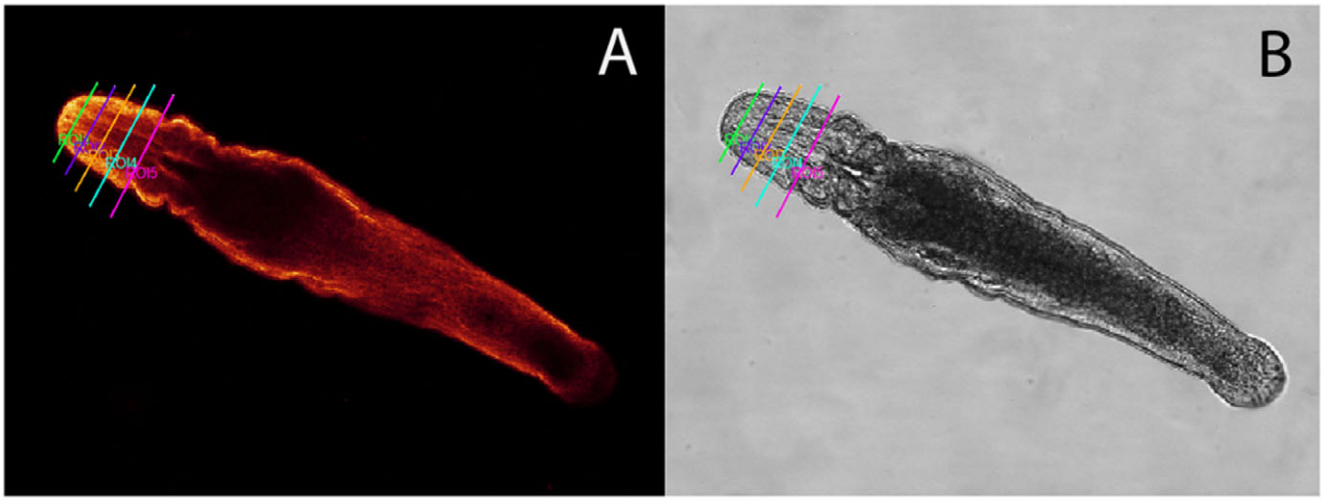

Fig. 1. Quantification analysis of the confocal images: a total of five transects were used for each of the animals under study (ROI, region of interest). These were always perpendicular to the longitudinal axis of the animal and were located in the areas with the highest fluorescence intensity. (A) Animal stained with MitoTracker Deep Red 633. (B) Transmission image of the same individual.

Fig. 1). The maximum value for each transect was obtained and the values of the five transects were averaged for each individual.

Experiments were repeated a minimum of two times (if results were identical) and up to four times, in order to confirm the differences between treatments. Data from the different replicas were pooled. However, as dye uptake by the animals varied on different days, the confocal settings needed to be adjusted in order to optimize the quality of the images taken. Thus, data normalization was required prior to pooling. Data were normalized by expressing all values within one experimental replica (10 worms) as a percentage of the maximum recorded value in that experiment. The maximum value was set to equal 100%. Statistical analyses were performed using SPSS 15.0 (SPSS Inc., Chicago, IL, USA). The resulting data were compared using ANOVA (followed by Student–Newman–Keuls *a posteriori* multiple comparison test) when data complied with the assumptions for parametric analyses. When this was not the case, Kruskal–Wallis tests were conducted.

RESULTS

Respiration measurements

For the normoxic treatment, P_{O_2}-dependent respiration rates were analyzed in a total of 10 pools, each consisting of 20 animals. Fig. 2 shows that respiration rates decreased rapidly (by 70%) between 19 and 12.5 kPa in the chamber. Below this P_{O_2}, *M. lignano* starts to regulate respiration down to a low critical P_{O_2}. Thus, for *M. lignano*, a first P_c was established at 13 kPa (P_{c1}), which marks the point at which the organisms are switching from conformity to regulation. Between 12.5 and ~3 kPa, the respiration rates of the worms were constant at around 0.064±0.001 nmol $O_2\,l^{-1}\,h^{-1}$ individual^{-1}. A second P_c appears at 1.36±0.32 kPa (P_{c2}), where respiration rates started to decrease again with declining P_{O_2}. Thus, the analysis reveals a high and a low P_c above which (P_{c1}) and below which (P_{c2}) the worms switch from regulating to conforming P_{O_2}-dependent respiration. The same pattern was observed for the animals that were previously maintained under anoxic conditions and subsequently reoxygenated. However, in the interval at which animals maintained constant respiration rates, values were significantly higher for the anoxia–reoxygenation group (0.083±0.001 nmol $O_2\,l^{-1}\,h^{-1}$ individual^{-1}) (F=458.23; P<0.001).

Activity observations

Normoxic and hyperoxic animals moved rapidly in the Petri dishes with a behavioral characteristic best described as unidirectional burst swimming. Consequently, for microscopic analysis at these high oxygenation levels, the worms had to be anesthetized with $MgCl_2$. In contrast, movement was drastically reduced in anoxia and often the worms started to swim in circles. Many worms were completely immobilized and displayed only epithelial cilia movements. Movements were completely reactivated by reoxygenation, with animals often reaching normoxic levels of activity after 1.5 h under reoxygenated conditions.

pH measurements

Staining with the pH-sensitive dye Ageladine-A (Fig. 3A; supplementary material Fig. S1A) indicated that the tissue pH levels in anoxic worms or those exposed to anoxia–reoxygenation were significantly more alkaline than those of normoxic and hyperoxic animals (ANOVA: F=10.38; P<0.001). Further estimation of the pH values (using the values of normoxic animals as a reference and assuming that non-specialized cells have a pH of 7.4) indicated a pH increase by ~0.10 units under near-anoxia and anoxia–reoxygenation conditions.

Staining with BCECF (supplementary material Fig. S1B) corroborated the general pattern obtained with Ageladine-A in which anoxic and reoxygenated individuals were significantly more basic than the normoxic and hyperoxic treatment groups (F=3.70; P<0.05) (Fig. 3B). As these results contradicted all our assumptions that animals exposed to near-anoxia should become, if anything, more acidic, we applied yet another approach with the wide-field fluorescence imaging microscope and BCECF. Again, animals under near-anoxia and anoxia–reoxygenation had the most alkaline values (supplementary material Fig. S2) (showing an average increase of 0.07 units), whereas the normoxia- and hyperoxia-treated worms had a tissue pH of 7.46.

Mitochondrial density and ψ_m-specific staining

MitoTracker staining indicated that most mitochondria were located in the animal's body wall in epithelial and muscle cells, as well as around the mouth area (Fig. 4). MitoTracker Green FM

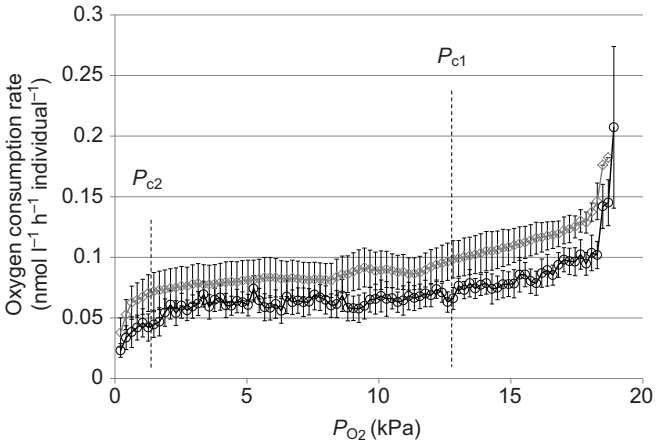

Fig. 2. Oxygen consumption rates of *Macrostomum lignano* at different environmental oxygen partial pressures (P_{O_2}). Values are pooled in 1% intervals. Black circles represent mean oxygen consumption rates for the 10 replicas, while gray diamonds represent the values obtained for animals that were maintained under anoxia and subsequently reoxygenated. Whiskers represent the s.e.m. P_{c1}, upper critical oxygen partial pressure; P_{c2}, low critical oxygen partial pressure.

(supplementary material Fig. S3A) stained different treatment groups with different intensities (K=54.09; P<0.000). Animals kept under hyperoxic conditions (40 kPa) were stained with the highest intensity, theoretically suggesting maximum mitochondrial density in hyperoxic worms, followed by individuals under normoxic conditions, which displayed less intensive staining (Fig. 5A). Animals kept in anoxia had the lowest staining values with MitoTracker green, and individuals that were maintained in anoxia and subsequently reoxygenated returned to the staining intensity recorded in normoxia.

To determine whether the significant differences between differently oxygenated groups were associated with oxygenation-dependent capacities for dye uptake, a second experiment was performed in which the animals were stained prior to exposure to the different oxygenation treatments. With this approach we obtained exactly the same group-specific pattern as in the first experiment in which the dye was applied following incubation at different oxygen levels. Therefore, we used MitoTracker Deep Red 633 in a third approach (supplementary material Fig. S3B), which did not produce a clear group-specific pattern. Pooled data from the four MitoTracker Deep Red 633 replicas yielded no significant differences among treatments (K=6.98; P=0.072) (Fig. 5B). High resolution confocal imagery confirmed staining of individual mitochondria in *M. lignano* cells (Fig. 6).

Staining with the dye JC-1 (supplementary material Fig. S3C) indicated significant differences in the chemiosmotic H^+ potential ($\Delta\psi_m$) across the mitochondrial inner membrane among treatments (F=15.14; P<0.001) (Fig. 5C). The smallest potentials were measured in animals exposed to normoxia and in those that were reoxygenated after 1.5 h of anoxic incubation. Animals exposed to hyperoxic and anoxic media showed significantly more red/green staining, indicating an elevated membrane potential, i.e. a stronger H^+ gradient.

Staining for ROS detection

Superoxide anion ($O_2^{\bullet-}$) concentrations were assessed with dihydroethidium (DHE) (supplementary material Fig. S4A). DHE staining was similar in animals exposed to anoxic, normoxic and hyperoxic conditions. Animals that were reoxygenated after a

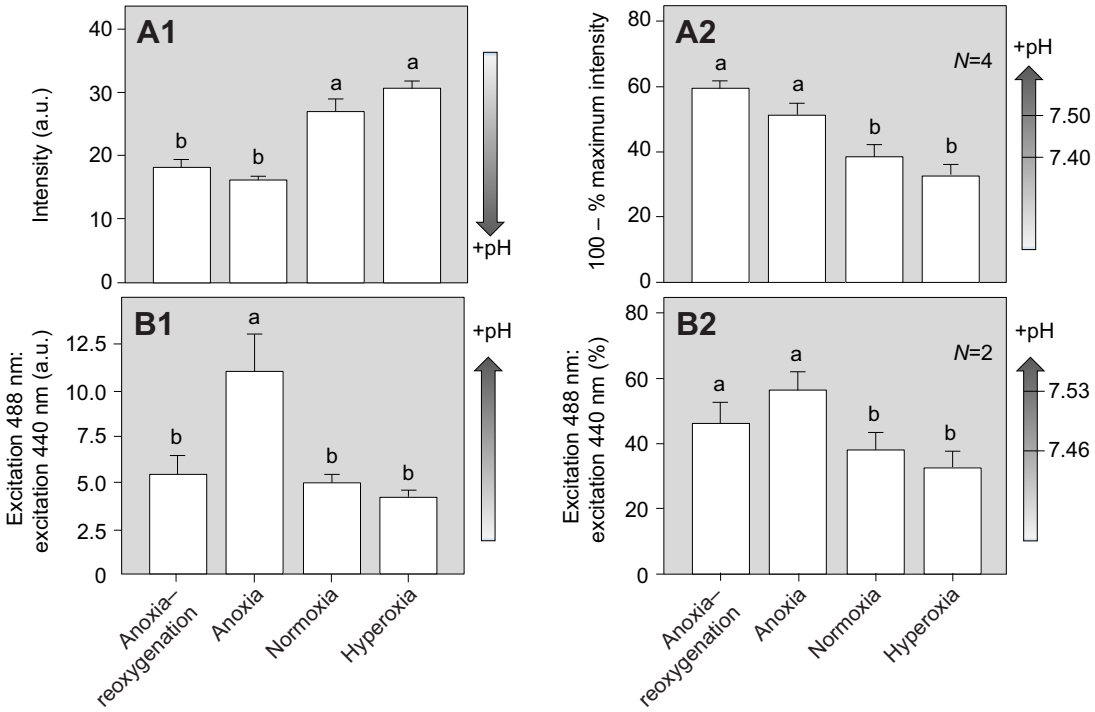

Fig. 3. Bar graphs showing the quantitative results obtained for pH measurements through (A) Ageladine-A staining (fluorescence intensity in arbitrary units, a.u.) and (B) BCECF staining (using the confocal microscope). (A1,B1) Results corresponding to one individual replica of the experiment. The pattern was consistent throughout the replicas in each case; therefore, data were normalized and pooled (see Materials and methods for more details). The corresponding results are shown in A2 and B2. Whiskers represent the s.e.m., N is the number of replicas. Groups with different lowercase letters are significantly different.

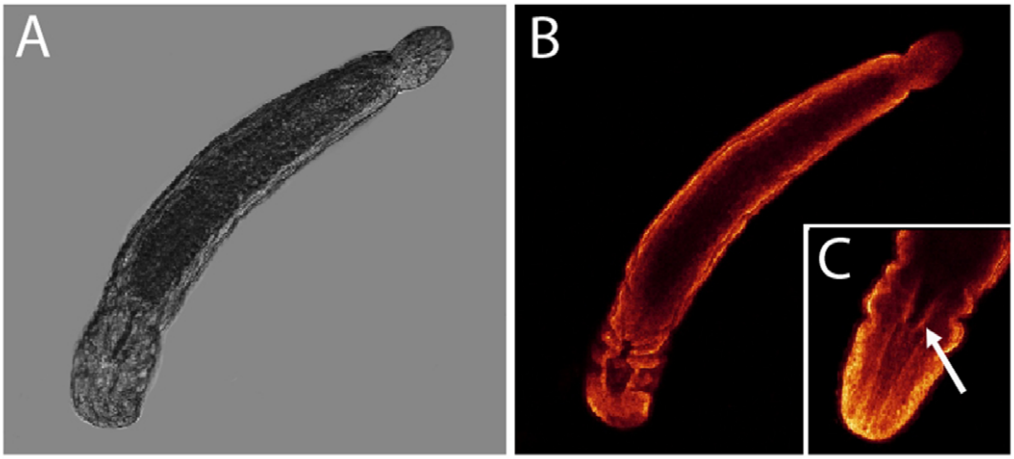

Fig. 4. Staining of *M. lignano* with MitoTracker Deep Red 633. (A) Transmission image of *M. lignano*. (B) MitoTracker Deep Red 633 fluorescence of the same individual showing how the highest mitochondrial densities can be found in the animal's body wall, in epithelial and muscle cells. (C) View of the head showing how a high mitochondrial density is also registered around the mouth (white arrow).

period of 1.5 h in anoxia had significantly increased DHE staining compared with all other groups (K=15.77; P<0.001) (Fig. 7A). Formation of other ROS species aside from $O_2•^-$ (H_2O_2, HOO• and $ONOO^-$) in *M. lignano* cells was assessed using C-H_2DFFDA (supplementary material Fig. S4B), which again showed important differences between treatments (K=80.82; P<0.000). The staining intensity decreased in the order anoxia–reoxygenation= hyperoxia>normoxia>near-anoxia (Fig. 7B), indicating ROS formation to decrease between hyperoxia and anoxia as expected.

Effects of superoxide dismutase and sodium diethyl-dithiocarbamate trihydrate on ROS staining

To scrutinize for the causes of the high DHE signal in anoxically incubated worms that should theoretically not be able to form $O_2•^-$, we applied a superoxide dismutase (SOD) solution (Sigma S-2515) and the SOD inhibitor sodium diethyl-dithiocarbamate trihydrate (SDT; Sigma D-3506) to anoxic animals stained with DHE (Fig. 8A). The first results with neither SOD nor SDT addition again led to significant DHE staining (above the background signal) in anoxically incubated specimens, although the values were significantly lower than those obtained with normoxic animals. SOD addition to anoxically incubated animals significantly reduced DHE staining, as $O_2•^-$ radicals were converted to H_2O_2 at higher rates. In contrast, addition of the SOD inhibitor SDT caused a 2-fold higher DHE fluorescence in anoxic animals compared with normoxically exposed animals, because fewer $O_2•^-$ radicals were converted to H_2O_2. Around 90% of the animals died under anoxic exposure with addition of SDT. After performing these tests to indirectly confirm the specificity of DHE for $O_2•^-$ detection, we assessed the effect of SOD addition on DHE and C-H_2DFFDA staining in an experiment with both dyes (Fig. 8B). Addition of SOD to the medium of anoxically incubated worms once again significantly reduced $O_2•^-$ in the DHE-stained worms compared with the normoxic control group. In contrast, SOD addition significantly increased C-H_2DFFDA staining, suggesting higher H_2O_2 concentrations in anoxically incubated SOD-supplemented animals than in normoxic controls.

DISCUSSION

Macrostomum lignano as a marine model organism for live imaging of physiological stress

In the present study we used living *M. lignano* individuals for the application of live imaging techniques. The transparency of this organism allowed an adequate and satisfactory measurement of the physiological parameters to be taken into account. Moreover, its small size also favored a fast and complete dye uptake, making live imaging with the whole animal possible.

P_{O_2}-dependent respiration in *M. lignano*

Respiration measurements in *M. lignano* cannot be conducted with single animals, and instead require batches of 20 specimens maintained in small volumes (90–100 µl) of liquid. As the respiration rates are extremely low, measurements need to be conducted in small glass or Plexiglas chambers without linings made of Teflon, which is known to be an oxygen binder.

Exposing *M. lignano* to decreasing oxygen concentrations during the respiration measurements showed that the worms maintain constant consumption rates between 3 and 12.5 kPa. This could indicate that this is the species' optimum range of respiration and the animals are actually regulating oxygen consumption, most likely by adjusting ciliary beat frequency. The velocity of ciliary pumping movements may determine the water flow over the body surface, which, in this species, also represents the respiratory epithelium. We could not quantify ciliary beat frequency in the present study; however, we did not observe remarkable differences in cilia movements under different oxygen concentrations. Although we cannot reject the hypothesis that animals are actively regulating ventilation through cilia beating, we should consider the possibility that such regulation does not exist and that, in fact, the results are driven by mitochondria saturation above 3 kPa and that the activity of an alternative oxidase could be responsible for the increase in O_2 consumption above 12.5 kPa. Regardless of the the reason, the range of constant respiration characterizes *M. lignano* as aerobic hypoxia-tolerant species. Similar P_{O_2}-dependent respiration patterns have been reported for other marine meiofauna such as oligochaetes (Giere et al., 1999) and the authors suggested this to be an important prerequisite for successfully inhabiting intertidal sediments with microscale spatial variations in the oxygen concentration.

Animals that were reoxygenated after enduring a 1.5 h period under anoxia showed a 30% increase in their respiration rates, probably due to the stress of the procedure.

Responses to high oxygen concentrations

$\Delta\psi_m$, and the way the ψ_m is affected by different oxygen concentrations, has mainly been addressed in mammalian cell cultures. For *M. lignano*, the JC1 measurements under normoxia and hyperoxia suggest that the increase in oxygen consumption is due not to mitochondrial uncoupling (opening of the mitochondrial

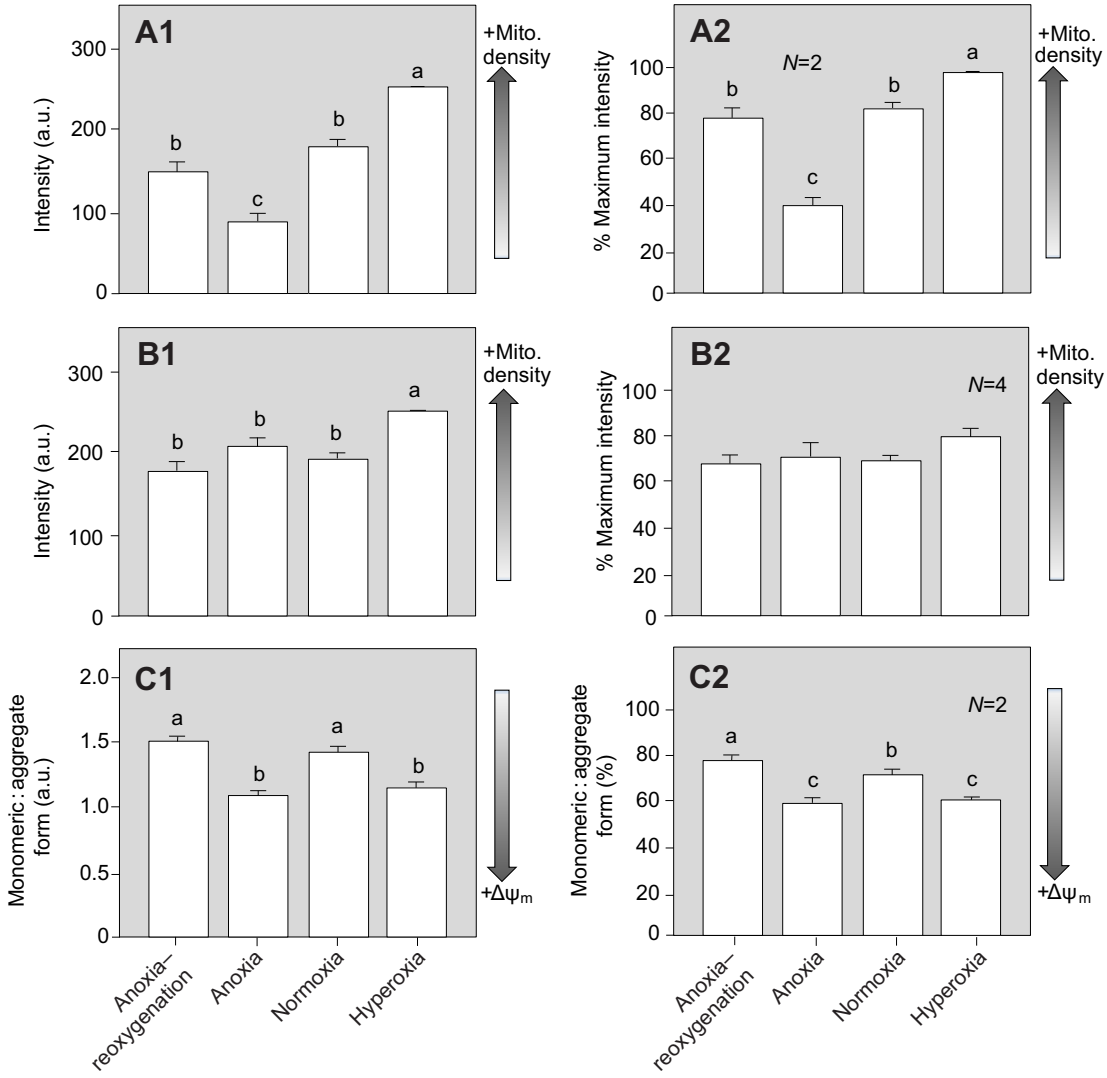

Fig. 5. Bar graphs showing the quantitative results obtained for the mitochondrial measurements through (A) MitoTracker Green FM and (B) MitoTracker Deep Red 633 staining for the assessment of mitochondrial density and (C) JC-1 staining for the determination of mitochondrial membrane potential ($\Delta\psi_m$). (A1,B1,C1) Results corresponding to one individual replica of the experiment. The pattern was consistent throughout the replicas in each case (except for MitoTracker Deep Red 633); therefore, data were normalized and pooled (see Materials and methods for more details). The corresponding results are shown in A2, B2 and C2. Whiskers represent the s.e.m., *N* is the number of replicas. Groups with different lowercase letters are significantly different.

membrane transmission pore) but to a more intensive respiration, electron flow, which causes increased $\Delta\psi_m$ in hyperoxically exposed worms. In contrast, mitochondrial uncoupling and a reduction of $\Delta\psi_m$ under hyperoxic conditions has been observed in mammalian microvascular cells (Sastre et al., 2000) and pneumocytes (Guthmann et al., 2005), which impressively highlights the difference between oxyconforming flatworms and oxyregulating mammalian cells. We did not observe aggregation of worms under normoxic/hyperoxic conditions indicating collective re-breathing as observed in ostracods when facing too high oxygen levels (Corbari et al., 2005). Indeed, a more thorough investigation of the migration or aggregation behavior of *M. lignano* within oxygenation structured micro-environments is warranted (Fenchel and Finlay, 2008). However, we did observe that the locomotory activity of the worms was conspicuously higher in normoxic and hyperoxic treatments, with no observable difference between the two oxygenation states. Thus, as in many other infaunal species (Abele et al., 1998), normoxic oxygen levels are already high for these plathyhelminths and their behavior indicates an attempt to reduce oxygenation in their sedimentary environment. This increased activity is fueled by the enhanced respiration above 12.5 kPa.

The C-H_2DFFDA measurements further indicate an increase in ROS (H_2O_2, HOO• and $ONOO^-$) production compared with normoxic worms, whereas no effect of hyperoxia on $O_2^{\bullet-}$ concentrations was observed in the DHE measurements. A cross-experiment in which we added either SOD or the SOD inhibitor STD to the medium confirmed that the DHE signal depends primarily on the amount of $O_2^{\bullet-}$ in the cells. The measurements with ROS-sensitive fluorophores therefore indicate that under hyperoxia the worms' SOD activity converts excess $O_2^{\bullet-}$ to H_2O_2. This conversion is abolished by the SOD inhibitor STD, which killed the animals when they were exposed under hyperoxic conditions. Mitochondrial production of ROS increases linearly with increasing oxygen concentration (Turrens et al., 1982), and hyperoxia has been shown to elicit oxidative stress and antioxidant responses in marine model organisms (Abele et al., 1998; Lushchak and Bagnyukova,

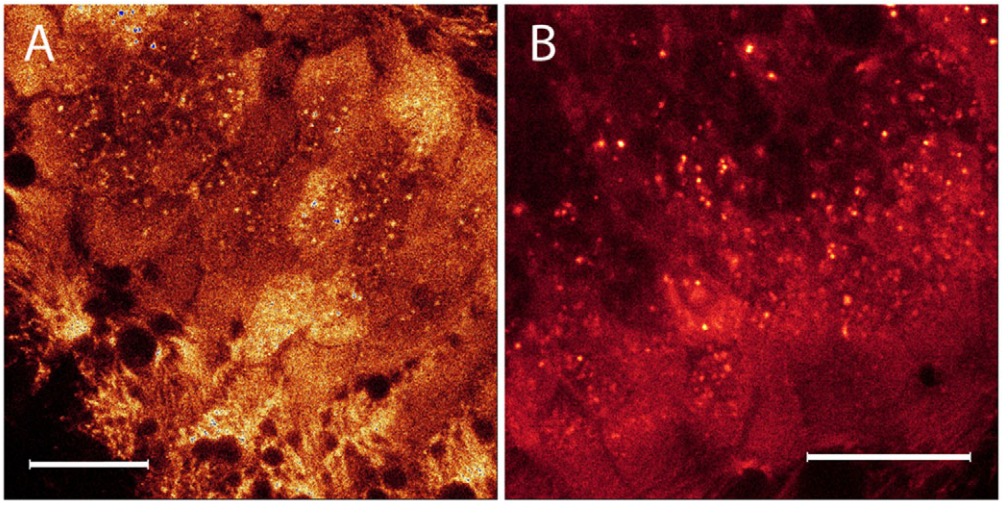

Fig. 6. High resolution fluorescence images of individual cells of *M. lignano* stained with MitoTracker Green FM under anoxic (A) and normoxic (B) conditions. Confocal imagery. Scale bars, 15 μm.

2006). Interestingly, 12.5 kPa is also the level at which mitochondria of the mammalian lung start to release H_2O_2 at a faster rate (compared with lower oxygen levels), indicating that antioxidant defenses are starting to be overwhelmed. It seems a bit far-fetched to suggest a common upper P_c for such distinct systems as meiofauna species and human lung epithelia, but the comparison illustrates the wide applicability of the hypothesis that in very diverse systems, P_{O_2} is kept at very low levels to prevent hyperoxic ROS production.

The pH of the tissue in hyperoxia was shown to be slightly more acidic than that in animals kept under normoxic conditions. This can result from various mechanisms such as intensified hydrolysis of ATP and oxidative inhibition of the Na^+/H^+ antiporter under enhanced oxidative stress, as reported for brain cells (Mulkey et al., 2004) and for crustaceans (Abele-Oeschger et al., 1997). Furthermore, in fish and some crustaceans, hyperoxic shocks can result in a reduction of ventilation rates, which causes extracellular acidosis (Gilmour and Perry, 1994; Gilmour, 2001; Wheatly and Toop, 1989).

Responses to anoxia and subsequent reoxygenation

Under anoxic conditions, *M. lignano* showed drastically reduced movements, presumably an energy-saving behavior in response to the lack of oxygen. A similar response to anoxia has been reported for a wide variety of invertebrate species, like bivalves (e.g. de Zwaan and Wijsman, 1976) or crustaceans (e.g. Hervant et al., 1995).

Even though we did not obtain numerical $\Delta\psi_m$ results, our data indicate that *M. lignano* mitochondria mount a stronger H^+ gradient under low oxygen concentrations than under normoxic conditions (Fig. 5). In normoxia, hypoxia-tolerant invertebrates have lower $\Delta\psi_m$ values than cold-blooded vertebrate and mammalian mitochondria

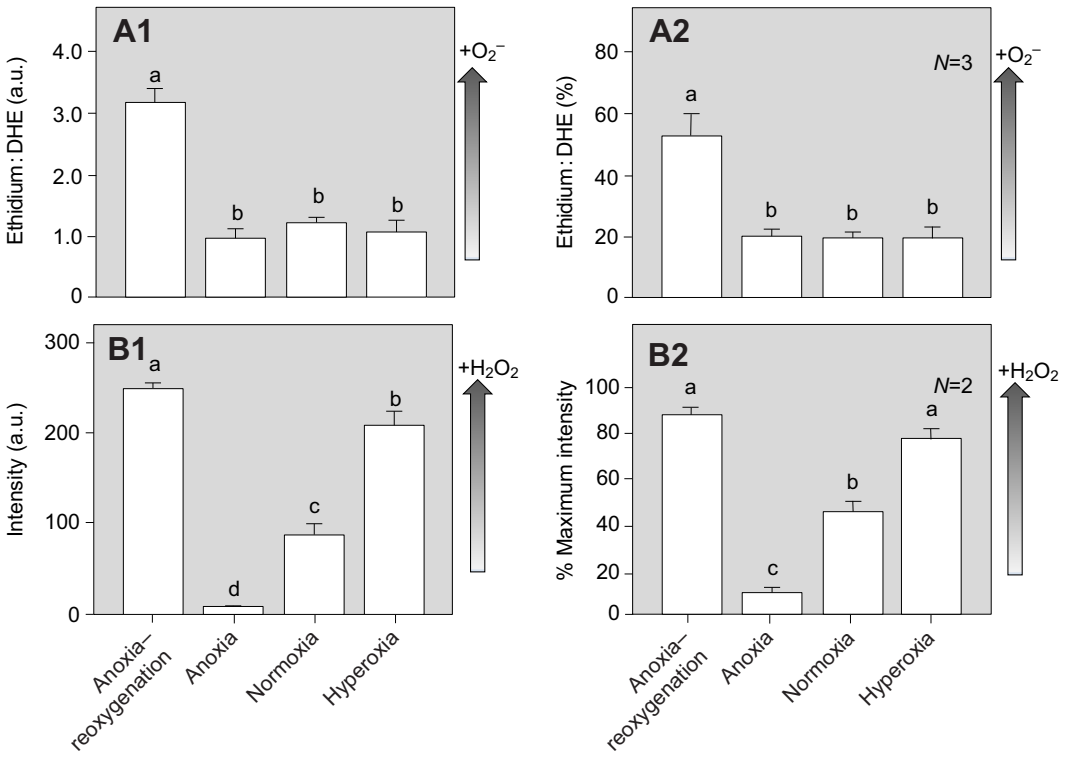

Fig. 7. Bar graphs showing the quantitative results obtained for reactive oxygen species (ROS) quantification through (A) dihydroethidium (DHE) and (B) C-H_2DFFDA staining. (A1, B1) Results corresponding to one individual replica of the experiment. The pattern was consistent throughout the replicas in each case; therefore, data were normalized and pooled (see Materials and methods for more details). The corresponding results are shown in A2 and B2. Whiskers represent the s.e.m., *N* is the number of replicas. Groups with different lowercase letters are significantly different.

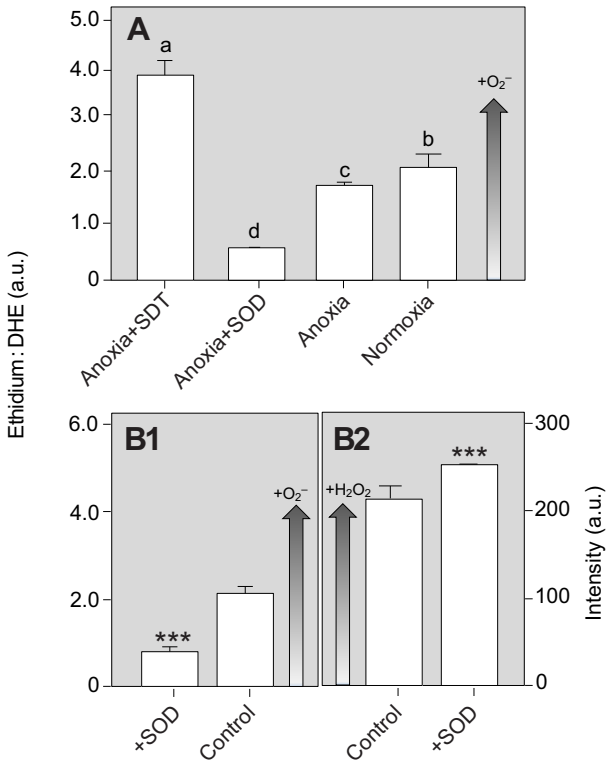

Fig. 8. Results on the effect of the inhibition of superoxide dismutase (SOD) under anoxic conditions. (A) Effect of SOD and the SOD inhibitor sodium diethyl-dithiocarbamate trihydrate (SDT) on anoxic animals. Groups with different lowercase letters are significantly different based on an *a posteriori* Student–Newman–Keuls multiple comparison test (K=27.41; P<0.001). (B) Effect of SOD on the concentrations of O_2^- (DHE values; b1) and H_2O_2 (C-H_2DFFDA values; b2) in anoxic animals. Whiskers represent the s.e.m. ***P<0.001.

(Abele et al., 2007; Brookes et al., 1998; Keller et al., 2004). Anoxic *M. lignano* also maintained high $\Delta\psi_m$ values as hyperoxic individuals, reinforcing the view that the species not only tolerates low oxygen concentration but also keeps up the mitochondrial proton gradient down to very low P_{O_2}. Under severely hypoxic to anoxic conditions, <1.5 kPa, oxygen consumption rates started to decline as oxygen became limiting. Maintenance of the high proton gradient would then be due to reduced energy expenditure including the complete absence of swimming mobility so that energetic requirements can be estimated to be minimal. This leads to the conservation of a high H^+ gradient because of a reduced phosphorylation activity and proton backflow at the ATPase.

However, anoxic animals also featured the most alkaline (least acidic) intracellular pH. This is paradoxical in the sense that for many organisms, cells and tissues, severe hypoxia has been demonstrated to lead to a decrease in cellular ATP, an increase of the free intracellular calcium concentration (e.g. Kristián and Siesjö, 1996) and acidification of extracellular and intracellular pH (e.g. Bickler, 1992). Only a few studies have observed hypoxic alkalization in cancer cells (for review, see Webb et al., 2011) and certain mammalian cells, in keeping with our results (Mitsufuji et al., 1995). Such an alkalization of the intracellular pH during anoxia could well be an adaptive strategy to avoid apoptosis, known to be associated with intracellular acidification (Lagadic-Gossmann et al., 2004; Matsuyama et al., 2000). But the question remains how such an increase of pH_i can be achieved. In cancer cells this has been associated with changes in the expression and/or activity of membrane transporters and ion pumps (see Webb et al., 2011). Other authors (e.g. Mitsufuji et al., 1995) suggested that the increasing pH values might be attributed to the activation of the Na^+/H^+ antiporter during hypoxia. As the Na^+ gradient across the cellular membrane is maintained by the Na^+/K^+-dependent ATPase, the driving force for the proton export by the Na^+/H^+ antiporter is an energy (ATP)-dependent process. The Na^+/H^+-antiporter exports intracellular protons, thus increasing pH_i and preventing acidosis until the cellular stores of ATP are exhausted. We have, however, demonstrated that ψ_m and potentially also the electron flow are maintained down to very low oxygen concentrations. As ATP requirements are reduced through the reduction of locomotion, we assume ATP to be available for the upkeep of the Na^+ gradient and therefore for stabilizing secondary active proton export during severe hypoxia, which would explain the less acidic values in our near-anoxia worms. As ATP concentration was not measured in the present study, this hypothesis cannot be corroborated. In future studies, ATP concentration and the involvement of membrane transporters in stabilizing intracellular pH should be tested by luminescence assays (ATP+APD) and using specific inhibitors for membrane transporters. Another factor that could theoretically contribute to the more alkaline pH values during periods of low oxygen concentration would be the decrease in ATP hydrolysis, which also involves H^+ release, because of the reduction of the worms' muscular activity. Although we consider hypoxic alkalinization to be an important new finding based on live imaging techniques and confirmed by the use of two different pH-sensitive dyes, further investigations of this phenomenon are recommended. While no exact calibration *in vivo* has yet been developed for Ageladine-A, BCECF has a reported accuracy of 0.07 pH units (Franck et al., 1996), which is within the range shift that we detected in the present study. Further experiments are planned to see whether pH_i alkalinization during hypoxia in the worms is accompanied by an extracellular acidification as observed in cancer cells (Webb et al., 2011).

The tenet that mitochondrial ROS formation increases linearly with oxygen concentration in cells (Turrens et al., 1982) is also disputable for the worms. Whereas H_2O_2 formation was in agreement with this theory, $O_2\bullet^-$ formation follows a different pattern: *M. lignano* individuals under near-anoxia showed similar $O_2\bullet^-$ concentrations to normoxic and hyperoxic animals. Under conditions of strict anoxia, and thus in the absence of oxygen, ROS can definitely not be produced. In consequence, under so-called anoxia, minimal traces of oxygen must still have been present, enough to cause some $O_2\bullet^-$ formation in the worms. It is still under debate whether ROS can be produced under hypoxia (Hermes-Lima et al., 1998; Hermes-Lima and Zenteno-Savín, 2002) and some evidence of this happening came first from direct ROS measurements (Vanden Hoek et al., 1997), followed by detection through resulting DNA damage (Englander et al., 1999). These results can, however, also be explained by the low K_m for O_2 of mitochondrial nitric oxide synthase, which would lead to production of NO, estimated to be around 5–10% of the normal steady rate of NO production (Alvarez et al., 2003). This NO may bind to and inhibit cytochrome oxidase, causing an increase in its K_m for oxygen and, consequently, an increased reduction of the upstream electron transporters such as complex I and III, and therefore enhanced formation of $O_2\bullet^-$ under hypoxic conditions (reviewed by Turrens, 2003). Further, NO can react with superoxide to form toxic peroxynitrite, which can lead to all sorts of macromolecular damage, including DNA damage, and presumably also induce antioxidant

systems. Based on the results obtained through the use of SOD and STD and their effect on anoxic individuals, we suggest that SOD might be inhibited during anoxia, which would additionally contribute to the high $O_2^{\bullet-}$ and the low H_2O_2 concentrations recorded under these conditions. For other invertebrate species such as clams, a decrease in SOD expression and activity has also been observed (Monari et al., 2005).

Effect of oxygenation on MitoTracker fluorescence

Mitochondria in *M. lignano* are mainly concentrated in muscular and epithelial cells, providing energy to the numerous cilia and for body contraction. Although the two MitoTracker dyes stained the same location, MitoTracker Green FM and MitoTracker Deep Red 633 gave significantly different results (Fig. 5; supplementary material Fig. S3) with respect to the comparison across treatments. Only with MitoTracker Green did we observe a decrease in staining under anoxia, which suggests fluorescence of this dye is negatively affected by anoxic exposure, even though it has been reported to be independent of membrane potential (Métivier et al., 1998). Some studies have demonstrated that this may not be true (Keij et al., 2000), and similar oxygenation-dependent patterns of JC-1 and MitoTracker Green FM in *M. lignano* strongly suggest that MitoTracker Green is indeed sensitive to $\Delta\psi_m$. In this case, MitoTracker Green FM cannot be considered as a useful probe for mitochondrial density in experiments involving variable tissue oxygenation. This is further supported by the fact that MitoTracker Deep Red 633 staining was independent of the experimental oxygenation state and can thus be considered a better tool for determining mitochondrial mass (Haugland, 2002) in this kind of experiment.

CONCLUSIONS

In an attempt to establish the platyhelminth *M. lignano* as an applicable whole-animal model for physiological investigations, we determined its peculiar physiological response to anoxic and hyperoxic exposure at different levels of cellular functioning. The worms are hypoxia tolerant and maintain the mitochondrial proton gradient and presumably also ATP levels during at least 2 h of anoxic exposure. Oxyconforming respiration below 3 kPa apparently satisfies the worm's maintenance metabolism and prevents the onset of cellular acidosis, while mobility ceases altogether and only ciliary movements are observable in anoxia and severe hypoxia. Elevated DHE fluorescence indicated superoxide formation in near-anoxia, which might be attributable to the diminished SOD activity at low tissue oxygenation. However, we suggest that *M. lignano* could also be an interesting model to study hypothetical respiratory chain superoxide formation at low tissue oxygenation under the possible influence of hypoxic NO formation. The response to hyperoxia also differed from that of mammalian systems, but aligned with other marine invertebrate infauna that increase respiration rates in a P_{O2}-dependent manner above an upper critical P_{c2}. This is often interpreted as an attempt to reduce excess oxygen in the animals' environment and could be characteristic of species that have successfully adapted to deal with the vagaries of environmental oxygenation in intertidal sediments.

LIST OF SYMBOLS AND ABBREVIATIONS

C-H2DFFDA	5-(and-6)-carboxy-2′,7 h-difluorodihydrofluorescein diacetate
DHE	dihydroethidium
NH-FSW	filtered sea water supplemented with 15 mmol l^{-1} Na-Hepes
P_c	critical oxygen pressure
pH_i	intracellular pH
P_{O_2}	oxygen partial pressure
ROS	reactive oxygen species
SDT	sodium diethyl-dithiocarbamate trihydrate
SOD	superoxide dismutase
$\Delta\psi_m$	mitochondrial membrane potential

ACKNOWLEDGEMENTS

The authors would like to thank Nelly Tremblay for her advice and comments on the respiration measurements and further data analysis, Stefanie Meyer for her valuable laboratory assistance and Peter Karuso, Achim Grube and Matthias Köck for kindly supplying the Ageladine-A used in the present study. Thanks also go to Dr V. Lushchak and one anonymous referee for the comments on the original manuscript.

AUTHOR CONTRIBUTIONS

All authors equally contributed to experimental design, data interpretation and writing of the manuscript. G.A.R.-I. performed the research and analysis of the data.

COMPETING INTERESTS

No competing interests declared.

FUNDING

This study was supported by Fundación Ramón Areces through a post-doctoral grant awarded to G.A.

REFERENCES

Abele, D., Großpietsch, H. and Pörtner, H. O. (1998). Temporal fluctuations and spatial gradients of environmental P_{O_2}, temperature, H_2O_2 and H_2S in its intertidal habitat trigger enzymatic antioxidant protection in the capitellide worm *Heteromastus filiformis*. *Mar. Ecol. Prog. Ser.* **163**, 179-191.

Abele, E., Philip, E., Gonzalez, P. M. and Puntarulo, S. (2007). Marine invertebrate mitochondria and oxidative stress. *Front. Biosci.* **12**, 933-946.

Abele-Oeschger, D., Sartoris, F. J. and Pörtner, H.-O. (1997). Hydrogen peroxide causes a decrease in aerobic metabolic rate and in intracellular pH in the shrimp crangon crangon. *Comp. Biochem. Physiol.* **117C**, 123-129.

Alvarez, S., Valdez, L. B., Zaobornyj, T. and Boveris, A. (2003). Oxygen dependence of mitochondrial nitric oxide synthase activity. *Biochem. Biophys. Res. Commun.* **305**, 771-775.

Bickler, P. E. (1992). Cerebral anoxia tolerance in turtles: regulation of intracellular calcium and pH. *Am. J. Physiol.* **263**, R1298-R1302.

Bickmeyer, U. (2012). The alkaloid Ageladine A, originally isolated from marine sponges, used for pH-sensitive imaging of transparent marine animals. *Mar. Drugs* **10**, 223-233.

Bickmeyer, U., Grube, A., Klings, K.-W. and Köck, M. (2008). Ageladine A, a pyrrole-imidazole alkaloid from marine sponges, is a pH sensitive membrane permeable dye. *Biochem. Biophys. Res. Commun.* **373**, 419-422.

Bode, A., Salvenmoser, W., Nimeth, K., Mahlknecht, M., Adamski, Z., Rieger, R. M., Peter, R. and Ladurner, P. (2006). Immunogold-labeled S-phase neoblasts, total neoblast number, their distribution, and evidence for arrested neoblasts in *Macrostomum lignano* (Platyhelminthes, Rhabditophora). *Cell Tissue Res.* **325**, 577-587.

Brookes, P. S., Buckingham, J. A., Tenreiro, A. M., Hulbert, A. J. and Brand, M. D. (1998). The proton permeability of the inner membrane of liver mitochondria from ectothermic and endothermic vertebrates and from obese rats: correlations with standard metabolic rate and phospholipid fatty acid composition. *Comp. Biochem. Physiol.* **119B**, 325-334.

Corbari, L., Carbonel, P. and Massabuau, J. C. (2004). How a low tissue O_2 strategy could be conserved in early crustaceans: the example of the podocopid ostracods. *J. Exp. Biol.* **207**, 4415-4425.

Corbari, L., Carbonel, P. and Massabuau, J.-C. (2005). The early life history of tissue oxygenation in crustaceans: the strategy of the myodocopid ostracod *Cylindroleberis mariae*. *J. Exp. Biol.* **208**, 661-670.

de Zwaan, A. and Wijsman, T. C. M. (1976). Anaerobic metabolism in Bivalvia (Mollusca). Characteristics of anaerobic metabolism. *Comp. Biochem. Physiol.* **54B**, 313-324.

Duggleby, R. G. (1984). Regression analysis of nonlinear Arrhenius plots: an empirical model and a computer program. *Comput. Biol. Med.* **14**, 447-455.

Egger, B., Ladurner, P., Nimeth, K., Gschwentner, R. and Rieger, R. (2006). The regeneration capacity of the flatworm *Macrostomum lignano* – on repeated regeneration, rejuvenation, and the minimal size needed for regeneration. *Dev. Genes Evol.* **216**, 565-577.

Englander, E. W., Greeley, G. H., Jr, Wang, G., Perez-Polo, J. R. and Lee, H.-M. (1999). Hypoxia-induced mitochondrial and nuclear DNA damage in the rat brain. *J. Neurosci. Res.* **58**, 262-269.

Fenchel, T. and Finlay, B. (1995). *Ecology and Evolution in Anoxic Worlds*. Oxford: Oxford University Press.

Fenchel, T. and Finlay, B. (2008). Oxygen and the spatial structure of microbial communities. *Biol. Rev. Camb. Philos. Soc.* **83**, 553-569.

Franck, P., Petitipain, N., Cherlet, M., Dardennes, M., Maachi, F., Schutz, B., Poisson, L. and Nabet, P. (1996). Measurement of intracellular pH in cultured cells by flow cytometry with BCECF-AM. *J. Biotechnol.* **46**, 187-195.

Fujita, M., Nakao, Y., Matsunaga, S., Seiki, M., Itoh, Y., Yamashita, J., Van Soest, R. W. M. and Fusetani, N. (2003). Ageladine A: an antiangiogenic matrixmetalloproteinase inhibitor from the marine sponge *Agelas nakamurai*. *J. Am. Chem. Soc.* **125**, 15700-15701.

Giere, O., Preusse, J. H. and Dubilier, N. (1999). *Tubificoides benedii* (Tubificidae, Oligochaeta) – a pioneer in hypoxic and sulfidic environments. An overview of adaptive pathways. *Hydrobiologia* **406**, 235-241.

Gilmour, K. M. (2001). The CO_2/pH ventilatory drive in fish. *Comp. Biochem. Physiol.* **130A**, 219-240.

Gilmour, K. and Perry, S. (1994). The effects of hypoxia, hyperoxia or hypercapnia on the acid-base disequilibrium in the arterial blood of rainbow trout. *J. Exp. Biol.* **192**, 269-284.

Guthmann, F., Wissel, H., Schachtrup, C., Tölle, A., Rüdiger, M., Spener, F. and Rüstow, B. (2005). Inhibition of TNFalpha in vivo prevents hyperoxia-mediated activation of caspase 3 in type II cells. *Respir. Res.* **6**, 10.

Haugland, R. P. (2002). *Handbook of Fluorescent Probes and Research Products*. USA: Molecular Probes Inc.

Hermes-Lima, M. and Zenteno-Savín, T. (2002). Animal response to drastic changes in oxygen availability and physiological oxidative stress. *Comp. Biochem. Physiol.* **133C**, 537-556.

Hermes-Lima, M., Storey, J. M. and Storey, K. B. (1998). Antioxidant defenses and metabolic depression. The hypothesis of preparation for oxidative stress in land snails. *Comp. Biochem. Physiol.* **120B**, 437-448.

Hervant, F., Mathieu, J., Garin, D. and Fréminet, A. (1995). Behavioral, ventilatory, and metabolic responses to severe hypoxia and subsequent recovery of the hypogean *Niphargus rhenorhodanensis* and the epigean *Gammarus fossarum* (Crustacea: Amphipoda). *Physiol. Zool.* **68**, 223-244.

Keij, J. F., Bell-Prince, C. and Steinkamp, J. A. (2000). Staining of mitochondrial membranes with 10-nonyl acridine orange, MitoFluor Green, and MitoTracker Green is affected by mitochondrial membrane potential altering drugs. *Cytometry* **39**, 203-210.

Keller, M., Sommer, A. M., Pörtner, H. O. and Abele, D. (2004). Seasonality of energetic functioning and production of reactive oxygen species by lugworm (*Arenicola marina*) mitochondria exposed to acute temperature changes. *J. Exp. Biol.* **207**, 2529-2538.

Kristián, T. and Siesjö, B. K. (1996). Calcium-related damage in ischemia. *Life Sci.* **59**, 357-367.

Ladurner, P., Schärer, L., Salvenmoser, W. and Rieger, R. M. (2005). A new model organism among the lower Bilateria and the use of digital microscopy in taxonomy of meiobenthic Platyhelminthes: *Macrostomum lignano*, n. sp. (Rhabditophora, Macrostomorpha). *J. Zool. System. Evol. Res.* **43**, 114-126.

Lagadic-Gossmann, D., Huc, L. and Lecureur, V. (2004). Alterations of intracellular pH homeostasis in apoptosis: origins and roles. *Cell Death Differ.* **11**, 953-961.

Lushchak, V. I. and Bagnyukova, T. V. (2006). Effects of different environmental oxygen levels on free radical processes in fish. *Comp. Biochem. Physiol.* **144B**, 283-289.

Matsuyama, S., Llopis, J., Deveraux, Q. L., Tsien, R. Y. and Reed, J. C. (2000). Changes in intramitochondrial and cytosolic pH: early events that modulate caspase activation during apoptosis. *Nat. Cell Biol.* **2**, 318-325.

Métivier, D., Dallaporta, B., Zamzami, N., Larochette, N., Susin, S. A., Marzo, I. and Kroemer, G. (1998). Cytofluorometric detection of mitochondrial alterations in early CD95/Fas/APO-1-triggered apoptosis of Jurkat T lymphoma cells. Comparison of seven mitochondrion-specific fluorochromes. *Immunol. Lett.* **61**, 157-163.

Mitsufuji, N., Yoshioka, H., Tominaga, M., Okano, S., Nishiki, T. and Sawada, T. (1995). Intracellular alkalosis during hypoxia in newborn mouse brain in the presence of systemic acidosis: a phosphorus magnetic resonance spectroscopic study. *Brain Dev.* **17**, 256-260.

Monari, M., Matozzo, V., Foschi, J., Marin, M. G. and Cattani, O. (2005). Exposure to anoxia of the clam, Chamelea gallina: II: Modulation of superoxide dismutase activity and expression in haemocytes. *J. Exp. Mar. Biol. Ecol.* **325**, 175-188.

Morrill, A. C., Powell, E. N., Bidigare, R. R. and Shick, J. M. (1988). Adaptations to life in the sulfide system: a comparison of oxygen detoxifying enzymes in thiobiotic and oxybiotic meiofauna (and freshwater planarians). *J. Comp. Physiol. B* **158**, 335-344.

Morris, J., Ladurner, P., Rieger, R., Pfister, D., Del Mar De Miguel-Bonet, M., Jacobs, D. and Hartenstein, V. (2006). The Macrostomum lignano EST database as a molecular resource for studying platyhelminth development and phylogeny. *Dev. Genes Evol.* **216**, 695-707.

Mouton, S., Willems, M., Braeckman, B. P., Egger, B., Ladurner, P., Schärer, L. and Borgonie, G. (2009). The free-living flatworm Macrostomum lignano: a new model organism for ageing research. *Exp. Gerontol.* **44**, 243-249.

Mulkey, D. K., Stornetta, R. L., Weston, M. C., Simmons, J. R., Parker, A., Bayliss, D. A. and Guyenet, P. G. (2004). Respiratory control by ventral surface chemoreceptor neurons in rats. *Nat. Neurosci.* **7**, 1360-1369.

Pfannkuche, O. and Thiel, H. (1988). Sample processing. In *Introduction to the Study of Meiofauna* (ed. R. P. Higgins and H. Thiel), pp. 134-145. Washington, DC: Smithsonian Institution.

Pfister, D., De Mulder, K., Phillip, I., Kuales, G., Hrouda, M., Eichberger, P., Borgonie, G., Hartenstein, V. and Ladurner, P. (2007). The exceptional stem cell system of Macrostomum lignano: screening for gene expression and studying cell proliferation by hydroxyurea treatment and irradiation. *Front. Zool.* **4**, 9.

Rosenberg, R., Hellman, B. and Johansson, B. (1991). Hypoxic tolerance of marine benthic fauna. *Mar. Ecol. Prog. Ser.* **79**, 127-131.

Sastre, J., Pallardó, F. V. and Viña, J. (2000). Mitochondrial oxidative stress plays a key role in aging and apoptosis. *IUBMB Life* **49**, 427-435.

Schärer, L., Sandner, P. and Michiels, N. K. (2005). Trade-off between male and female allocation in the simultaneously hermaphroditic flatworm *Macrostomum* sp. *J. Evol. Biol.* **18**, 396-404.

Silver, R. B. (2003). Ratio imaging: measuring intracellular Ca^{2+} and pH in Living Cells. In *Methods in Cell Biology*, Vol. 72 (ed. W. Leslie and M. Paul), pp. 369-387. Academic Press.

Tang, P.-S. (1933). On the rate of oxygen consumption by tissues and lower organisms as a function of oxygen tension. *Q. Rev. Biol.* **8**, 260-274.

Thomas, J. A., Buchsbaum, R. N., Zimniak, A. and Racker, E. (1979). Intracellular pH measurements in Ehrlich ascites tumor cells utilizing spectroscopic probes generated in situ. *Biochemistry* **18**, 2210-2218.

Tinson, S. and Laybourn-Parry, J. (1985). The behavioural responses and tolerance of freshwater benthic cyclopoid copepods to hypoxia and anoxia. *Hydrobiologia* **127**, 257-263.

Turrens, J. F. (2003). Mitochondrial formation of reactive oxygen species. *J. Physiol.* **552**, 335-344.

Turrens, J. F., Freeman, B. A., Levitt, J. G. and Crapo, J. D. (1982). The effect of hyperoxia on superoxide production by lung submitochondrial particles. *Arch. Biochem. Biophys.* **217**, 401-410.

Vanden Hoek, T. L., Li, C., Shao, Z., Schumacker, P. T. and Becker, L. B. (1997). Significant levels of oxidants are generated by isolated cardiomyocytes during ischemia prior to reperfusion. *J. Mol. Cell. Cardiol.* **29**, 2571-2583.

Webb, B. A., Chimenti, M., Jacobson, M. P. and Barber, D. L. (2011). Dysregulated pH: a perfect storm for cancer progression. *Nat. Rev. Cancer* **11**, 671-677.

Wetzel, M. A., Fleeger, J. W. and Powers, S. P. (2001). Effects of hypoxia and anoxia on meiofauna: a review with new data from the Gulf of Mexico. *Coastal and Estuarine Studies* **58**, 165-184.

Wheatly, M. G. and Toop, T. (1989). Physiological responses of the crayfish *Pacifastacus leniusculus* to environmental hyperoxia: II. Role of the antennal gland in acid–base and ion regulation. *J. Exp. Biol.* **143**, 53-70.

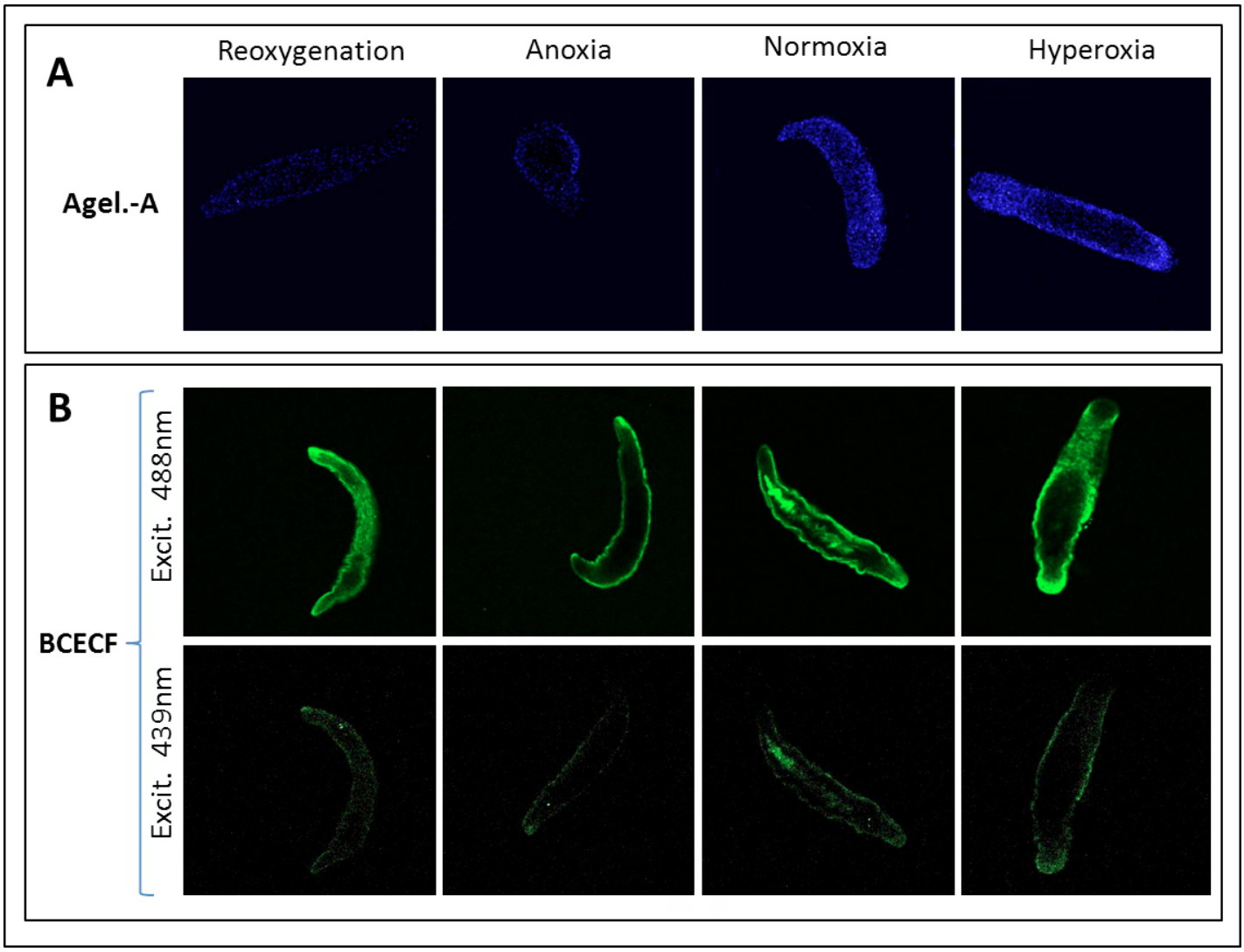

Fig. S1. Representative fluorescence images obtained during pH measurements under the confocal microscope for each of the treatments considered. (A) Ageladine-A staining. (B) BCECF staining.

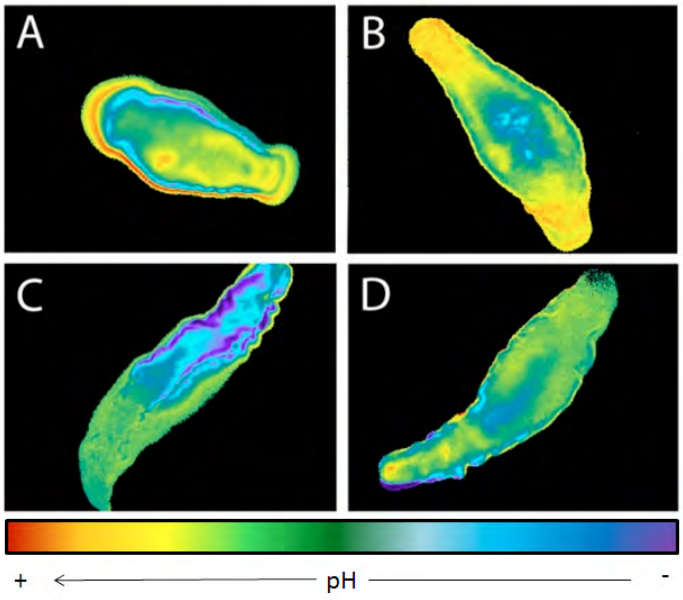

Fig. S2. Wide-field fluorescence imaging of *M. lignano* individuals stained with BCECF under the four treatments considered in the study: (A) anoxia followed by reoxygenation, (B) near-anoxia, (C) normoxia and (D) hyperoxia.

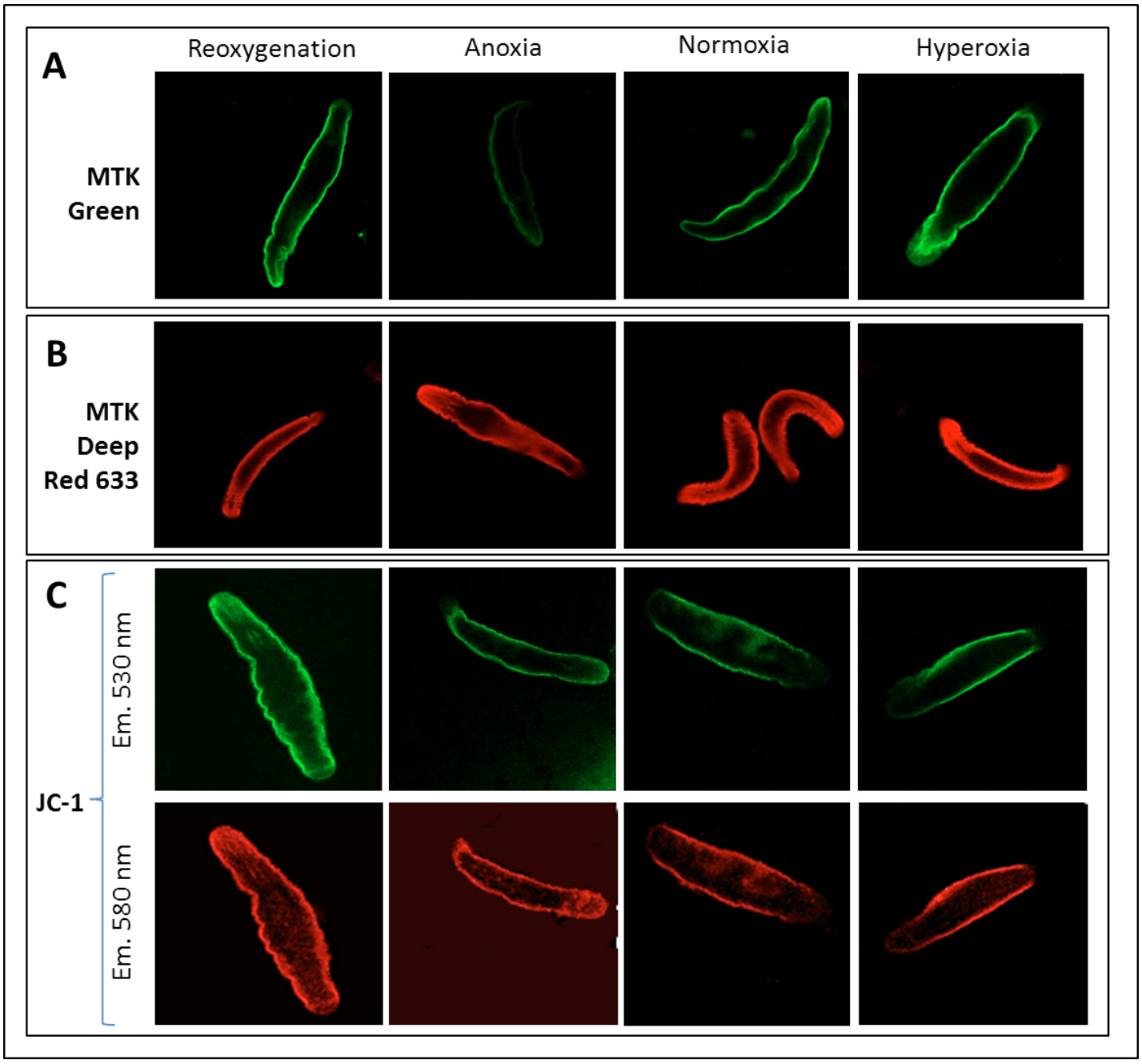

Fig. S3. Representative fluorescence images obtained during mitochondrial measurements under the confocal microscope for each of the treatments considered. (A) MitoTracker Green FM and (B) MitoTracker Deep Red 633 were used for mitochondrial mass estimation; (C) JC-1 was used for $\Delta\psi_m$ calculation.

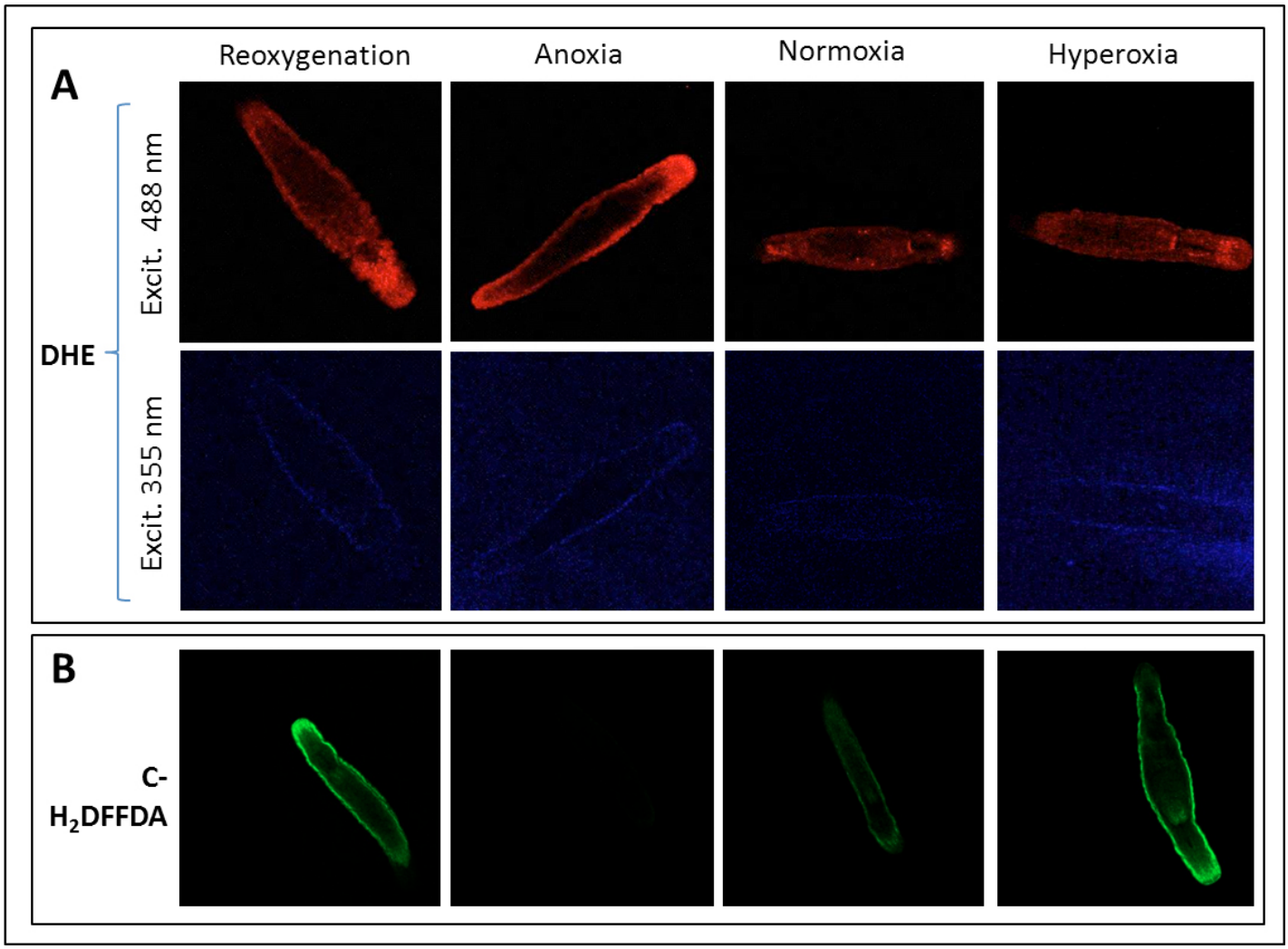

Fig. S4. Representative fluorescence images obtained during ROS quantification under the confocal microscope for each of the treatments considered. (A) DHE and (B) C-H_2DFFDA were used for O_2• and H_2O_2 quantification, respectively.